



HAL
open science

Coupling of electrochemical techniques to study copper corrosion inhibition in 0.5 mol L⁻¹ NaCl by 1-pyrrolidine dithiocarbamate

Wafaa Qafsaoui, M.W. Kendig, Hubert Perrot, Hisasi Takenouti

► **To cite this version:**

Wafaa Qafsaoui, M.W. Kendig, Hubert Perrot, Hisasi Takenouti. Coupling of electrochemical techniques to study copper corrosion inhibition in 0.5 mol L⁻¹ NaCl by 1-pyrrolidine dithiocarbamate. *Electrochimica Acta*, 2013, 87, pp.348-360. 10.1016/j.electacta.2012.09.056 . hal-00803261

HAL Id: hal-00803261

<https://hal.sorbonne-universite.fr/hal-00803261>

Submitted on 31 Mar 2015

HAL is a multi-disciplinary open access archive for the deposit and dissemination of scientific research documents, whether they are published or not. The documents may come from teaching and research institutions in France or abroad, or from public or private research centers.

L'archive ouverte pluridisciplinaire **HAL**, est destinée au dépôt et à la diffusion de documents scientifiques de niveau recherche, publiés ou non, émanant des établissements d'enseignement et de recherche français ou étrangers, des laboratoires publics ou privés.

Coupling of electrochemical techniques to study copper corrosion inhibition in 0.5 mol L⁻¹ NaCl by 1-pyrrolidine dithiocarbamate

W. Qafsaoui^{a,1*}, M.W. Kendig^b, H. Perrot^{c,d,1}, H. Takenouti^{c,d,1}

^a Laboratoire de l'Eau et de l'Environnement, Faculté des Sciences d'El Jadida, BP 20, 24000 El Jadida, Morocco. wqafsaoui@gmail.com

^b Kendig Research Associates LLC, 496 Hillsborough, Thousand Oaks, CA 91361. USA, martin.kendig@verizon.net

^c CNRS, UPR15 du CNRS, LISE, Case 133, 4 Place Jussieu, 75252 Paris Cedex 05, France. hubert.perrot@upmc.fr, hubert.perrot@upmc.fr

^dUPMC, LISE, Case 133, 4 Place Jussieu, 75252 Paris Cedex 05, France. hubert.perrot@upmc.fr, hisasi.takenouti@upmc.fr

Abstract

In this work, as for the preliminary step to the protection of Al 2xxx alloys, the anticorrosion effect of environmentally friendly 1-pyrrolidine dithiocarbamate (PDTC) on Cu was investigated by combining various electrochemical methods in addition to SEM-EDS analyses and gravimetric measurements. The Cu / PDTC system was used as a model to simulate the inhibition of Cu-rich particles contained in Al 2xxx alloys. The corrosion test solution was 0.5 mol L⁻¹ NaCl in presence of 10⁻⁴, 10⁻³, or 10⁻² mol L⁻¹ PDTC. The immersion time of the copper electrode was extended generally up to 24 hours. By EQCM measurements, a marked protective effect of PDTC was observed for the highest PDTC used, and corroborated by voltammetry and EIS measurements. The cathodic reduction under constant current allowed determining the corrosion products remaining on the copper surface in terms of electrical charge. The protective effect of PDTC was explained by the formation of highly stable compounds on the copper surface, which decreases the rate of both anodic dissolution and oxygen reduction reaction.

Key words: EIS; EQCM; Oxygen Reduction Reaction; Surface film; Voltammetry

¹ ISE member

* Corresponding author: Fax: +212.523 34 21 87; E-mail: wqafsaoui@gmail.com

1. Introduction

The 2xxx series of aluminium alloys obtained by addition of large quantities of copper to pure aluminium exhibit excellent mechanical properties. This copper addition leads to a heterogeneous microstructure constituted by copper rich precipitates. However, although the high strength acquired, these alloys suffer corrosion damages due to the formation of galvanic cells between the aluminium matrix and copper rich-particles, particularly in chloride-containing medium [1,2]. These precipitates provide surfaces where oxygen can readily be reduced; therefore they constitute the cathodic area. Treatments involving the use of chromates and dichromates provide a highly efficient corrosion protection for aluminium alloys, particularly those containing copper [3]. However, chromate solutions cause health and environment risks because hexavalent chromium compounds have an important toxic effect and are carcinogenic. Efforts are then made to replace Cr(VI) by non-toxic compounds able to specifically protect Cu-rich particles. Current attention of researchers is focused on the inhibition of electrochemical processes, especially the oxygen reduction reaction (ORR), on copper rich-particles to reach an action quite similar to that of Cr(VI). Corrosion inhibitors for copper, such as organic molecules, could then be considered as alternatives [4,5].

Corrosion protection of metals by organic compounds depends mainly on the chemical structure of the inhibitor and its adsorption mode. Several groups of heterocyclic organic compounds have been reported to exert inhibitive effect on copper corrosion in different media [6-9]. Benzotriazole (BTAH) is one of the most famous inhibitors for copper and copper alloys [10-14]. In previous works [4,5], we showed that BTAH and 3-amino 1,2,4-triazole (ATA) inhibit the dissolution associated with Cu-rich particles by the formation of protective complexes upon the particles. In the same way, Williams et al [15] showed that organic and inorganic anions inhibit pitting corrosion of Al 2024 T3 alloy in 5% NaCl, by film formation on Cu-rich particles and / or precipitation of copper cations. However, these

compounds that act efficiently on Cu-rich particles are more or less toxic or noxious. In line with environmental protection requirements, toxic inhibitors that are widely used in industrial processes should be replaced with new environmentally friendly inhibitors.

Certain dithiols as 1-pyrrolidine dithiocarbamate (PDTC) inhibit ORR on Cu electrodes [16-18]. PDTC is a non-toxic product widely used in agricultural and medical applications [19] and may therefore provide an alternative to chromate-based inhibitors. PDTC was shown to inhibit corrosion of steel water pipes in different corrosion media [20]. Recent works on copper corrosion inhibition in 0.5 mol L^{-1} HCl by PDTC [21] showed that this compound is able to interact with copper to form a self-assembled monolayer allowing a high inhibition efficiency to be obtained (up to 95.3 %). Moreover, the authors showed that the sulphur atoms in the PDTC are the main active sites for the adsorption on the copper surface.

Our previous works [22] with PDTC showed, besides inhibition of ORR, the formation of a highly barrier film on copper in 0.2 g L^{-1} NaCl. This film constitutes a partially blocking surface to diffusion-limited reactions. Preliminary tests on 2024-T3 aluminium alloy [23] showed that PDTC decreases considerably anodic and cathodic current densities of the alloy in 0.2 g L^{-1} NaCl and shifts the open circuit potential towards cathodic values. However, PDTC has no inhibitive effect on pure Al in the same medium suggesting that PDTC interacts solely with the Cu-rich particles. To understand this interaction in more detail, it seemed important to estimate its action on copper in chloride media.

It is clear that the main objective of this work is to study Cu / PDTC system to understand the inhibitive behaviour of PDTC on Al 2xxx alloys in chloride media. However, this work is in itself relevant to inhibition of pure copper since corrosion inhibition of Cu by PDTC is scarcely reported in the literature.

By selecting PDTC, the major aim of the present work focuses on its influence on general corrosion of copper in 0.5 mol L^{-1} NaCl solution. Electrochemical experiments were carried

out to study the behaviour of the copper / solution interface in the presence of different concentrations of PDTC.

2. Experimental

2.1 Electrodes

The disk electrodes were made of copper cylinder rod (Goodfellow) of 5 mm in diameter. First, the lateral part of the cylinder was covered with cataphoretic paint (PGG W975 + G323) to avoid the electrolyte infiltration. The copper rod was then embedded into allylic resin or thermal shrinking sheath. The electrode surface was abraded, just before experiments by rotating emery paper up to 1200 grade under water flow, and then rinsed abundantly with deionised water.

For EQCM (Electrochemical Quartz Crystal Microbalance) experiments, two 0.2 cm² gold electrodes were vapour deposited on both the free faces of the quartz crystal blade to impose electrical field for oscillation. One of the faces was used as working electrode and, for this purpose copper was electro-deposited on the gold electrode from 0.5 mol L⁻¹ CuSO₄ + 0.5 mol L⁻¹ H₂SO₄ solution by a cathodic current of 30 mA cm⁻² for 6 min. In these conditions, the mass of deposited copper was about 3.5 mg cm⁻² or 4 μm thick. The deposit thus obtained was polycrystalline and compact. The nominal resonant oscillation frequency of quartz blade was 6 or 9 MHz. For 6 MHz quartz crystals, experimental calibration measurements gave 1 μg cm⁻² of the mass loss corresponding to the increase of oscillation frequency of 164 Hz [24-26]. Measurements were carried out with a lab-made device and monitoring program.

The working electrode was set close to the centre of the electrolyzing cell, and under stationary conditions, i.e. without any electrolyte stirring.

The reference electrode was a calomel electrode in saturated KCl (SCE). All potentials are referred as measured, without any correction of liquid junction potential. No correction for the ohmic drop was made since its effect is negligible for analyses of polarization curves. The counter electrode was a platinum grid of large surface area set close to the cell wall.

2.2 Electrolytes

The blank corrosion test solution was 0.5 mol L⁻¹ NaCl to which 10⁻⁴, 10⁻³, or 10⁻² mol L⁻¹ of PDTC was added as inhibitor. 100 mL of electrolyte was used for each experiment. The corrosion test was carried out without purging of dissolved oxygen and maintained at 20 °C. The molecular structure of PDTC is presented in Fig. 1. This molecule has three heteroatoms; one nitrogen and two sulphur atoms, thus possesses high possibilities of adsorption on metal surface conferring a good candidate for the corrosion inhibitor. This substance is considered an irritant but is otherwise innocuous [27].

2.3. Surface analysis

The surface morphology of copper electrode was investigated with a LEICA STEREOSCAN 440 scanning electron microscope (SEM) and element analyses were performed with an energy dispersive X-ray analyzer (EDX; Princeton Gamma-Tech[®]).

2.4 Electrochemical measurements

For coulometric experiments to evaluate the amount of copper corrosion products accumulated at the electrode surface, the specimen was first immersed in the corrosion test solution without or with PDTC during 1 or 24 hours at the open circuit conditions. Then, the copper electrode was immediately rinsed with deionised water and transferred to a borate buffer solution; 10⁻² mol L⁻¹ H₃BO₃+ 10⁻² mol L⁻¹ Na₂B₄O₇ (pH 9). In this solution, corrosion products were reduced at the current density equal to -50 μA cm⁻². The solution was purged of

oxygen by Ar bubbling before the experiments and then Ar was flowed over the electrolyte surface [28].

Polarization measurements were carried out in a conventional three-electrode cell. The disk working electrode was stationary and faced towards the cell bottom. Electrochemical measurements were performed after 1 or 24 hours immersion (if not specified differently) in the test solution with or without the inhibitor.

The voltammetric and impedance measurements were carried out using a Gamry potentiostat / galvanostat Model FAS-1 or 300C. Polarization curves were plotted from two independent measurements in a new test solution for each run: one from the open circuit potential towards about -1.5 V after 1 or 24 hours immersion period, and another from the open circuit potential to about +1.5 V at the potential scan rate of 1 mV s^{-1} . 5 to 10 replica experiments were carried out for each experimental condition. In spite of careful experimental manipulations, the open circuit corrosion potentials were not as reproducible as expected, and changed by about ± 50 mV. Therefore, instead of the mean value, the most representative one was presented in this paper.

The impedance measurements were performed with $10 \text{ mV}_{\text{rms}}$ from 100 kHz to 10 mHz by 10 points per decade during 48 hours. For parameter regression calculation procedure, sometimes high frequency data (for instance beyond 40 kHz) were deleted since some instrumental and systematic error was observed, especially when the impedance spectrum exhibited a high capacitance (typically greater than $10 \text{ }\mu\text{F}$) at high frequency domain.

3. Results and discussion

To characterise the inhibitive effect of PDTC on the copper electrode, first the gravimetric measurements were carried out. Then, the amount of corrosion products accumulated on the copper electrode was evaluated by coulometry at constant cathodic current. These

experiments were followed by voltammetric measurements to determine the effect of PDTC on cathodic and anodic reactions. Finally the impedance spectroscopy was used to estimate the time change of inhibitive effect of PDTC at different concentrations.

3.1 EQCM

The results of gravimetric measurement obtained by Electrochemical Quartz Crystal Microbalance (EQCM) are presented in Fig. 2. Two behaviours can be distinguished:

- For the blank test solution and 10^{-4} mol L⁻¹ PDTC, the mass decreased continuously with time, indicating that the dissolution of Cu from the electrode surface is the predominant effect. However, an attentive examination of this curve with enlarged scale at the very beginning of the electrode immersion, revealed a slight mass increase observed in the blank test solution as illustrated in the insert. It can be also noticed that beyond 12 hours of immersion, the slope of Δm with respect to time t became steeper for the blank; whereas, the rate of Δm change decreased in the presence of 10^{-4} mol L⁻¹ of PDTC. Hence, it can be assumed that at this concentration of PDTC, its protective effect is insufficient, and only slows down the dissolution rate.
- For higher PDTC concentration (10^{-3} and 10^{-2} mol L⁻¹), a global mass increase was observed, and $\Delta m/\Delta t$ approached zero more or less quickly depending on the concentration. When 10^{-2} mol L⁻¹ PDTC was present, the mass increase was faster in an early immersion period but becomes slower after half an hour. In presence of 10^{-3} mol L⁻¹ PDTC, the mass increase was slower than the most concentrated solution but this increase lasted for longer period of time, during ca. 6 hours. Consequently, the mass increase after 24 hours of immersion was greater in 10^{-3} mol L⁻¹ solution likely due to the formation of CuCl layer with some PDTC molecules at the electrode surface.

From these curves, the rate of mass change (that may directly be associated with the corrosion rate) was estimated from linear regression calculation for early (1 to 4 hours) and the late immersion period (21 to 24 hours). The time intervals at which these calculations were performed were indicated by dotted lines.

- For low PDTC concentrations, it was postulated that the copper dissolves as cuprous ion according to the following overall reaction [29-30]:



It is important to remark that both Cu_2O and CuCl [31] layers may form upon the electrode surface as can be estimated from an early mass change in the blank test solution. It is important to emphasize that the estimation of the corrosion current density (j_{corr}) by $\Delta m(t)$ curve postulates therefore that the amount of the surface species reached its steady state value. If the accumulation of the corrosion products is taking place together with the Cu dissolution, the corrosion current density evaluated from the rate of mass change should be underestimated. This may particularly be true for a short immersion period as seen in the insert. Indeed, during the first minutes of immersion, Cu_2O and CuCl formation seems to overcome copper dissolution.

- In presence of higher inhibitor concentration, it is assumed that the mass increase is due only to the formation of CuCl layer [29], stabilized by PDTC.



The mass change is then expressed in terms of j_{corr} by applying the Faraday law. It is worth to notice however that the presence of PDTC was neglected though some SEM pictures showed, as shown below, few crystals.

The electrode mass remains constant, in the limit of the measurement resolution, above 12 hours in presence of 10^{-3} mol L⁻¹ PDTC and one hour for 10^{-2} mol L⁻¹ PDTC. That is, neither the dissolution of Cu through CuCl_2^- nor the formation of surface film become negligible.

For the first case (Eq. 1), only Cu atoms leaving the electrode were taken into account as the origin of the mass loss, whereas for the latter (Eq. 2), only Cl forming CuCl was involved. The Cu atoms were just transferred from the metal substrate to the surface layer, thus the mass balance is naught. Table 1 summarizes the rate of mass change and the corrosion current density tentatively estimated with the hypotheses above. It is important to notice that in this consideration, the formation of Cu₂O attested by coulometric measurements is neglected (see paragraph 3.3).

From this table, it can be remarked that the corrosion rate decreased with immersion period and the corrosion current density in presence of 10^{-2} mol L⁻¹ PDTC was about 60 nA cm⁻²; the inhibitive efficiency was as high as 99 %.

From EQCM measurements it can be then concluded that the action of PDTC at low contents consists only in slowing down the copper dissolution rate. However, at high concentration, PDTC has a good inhibiting efficiency due to the stabilization of the surface layers. This effect is obtained easily and quickly for 10^{-2} mol L⁻¹ but lasts 6h for 10^{-3} mol L⁻¹. Besides, it should be noted that these results were obtained assuming that corrosion products reached their steady-states. To correct these oversimplifications, the corrosion products accumulated on the electrode surface will be determined with cathodic reduction (section 3.3).

3.2 SEM observation and EDX analysis

Surface observations and analysis were performed on copper electrode (disk made of copper rod) after 24 hours immersion in 0.5 mol L⁻¹ NaCl containing 10^{-4} or 10^{-2} mol L⁻¹ of PDTC.

SEM images show a markedly attacked surface in $0.5 \text{ mol L}^{-1} \text{ NaCl} + 10^{-4} \text{ mol L}^{-1} \text{ PDTC}$ (Fig. 3a). Two areas can be distinguished on the surface, area covered with a dark and coarse film and bare surface with ridge of abrading. EDX analysis (Fig. 3b) indicated the presence of S and Cl atoms at the dark film suggesting that this film is likely composed mainly of CuCl and Cu-PDTC complexes. However, this film is poorly adherent and as concluded from EQCM results, it has poor barrier property to protect the copper substrate from corrosion (Fig. 2).

As for the copper immersed in $0.5 \text{ mol L}^{-1} \text{ NaCl} + 10^{-2} \text{ mol L}^{-1} \text{ PDTC}$, Fig. 4a shows a ridge surface by abrading and some crystals above. In contrast to the case presented above, the ridge surface is also covered by a film likely formed of PDTC with CuCl but extremely thin since EDX analysis showed the presence of S with Cu. This film is too thin to perform a quantitative EDX elemental analysis. As for the crystals, the same elements are detected but S/Cu ratio is higher indicating a higher PDTC content. (Figs 4b and 4c). PDTC will interact with copper atoms to form a complex on the electrode. Then one might conclude that a barrier film is formed on copper in presence of $10^{-2} \text{ mol L}^{-1}$ of PDTC in agreement with the results obtained by EQCM.

3.3 Coulometry under cathodic current

In order to evaluate the species accumulated on the Cu electrode during a short period (1 h) or 24 hours of immersion, coulometric measurements were performed. Fig. 5 presents the results obtained by galvanostatic reduction of surface layers. Whatever the length of the immersion period, two potential plateaux can be seen clearly for the electrode immersed in the blank test solution:

- The first one is located at about $-0.58 \text{ V}_{\text{SCE}}$, and this potential is close to that reported to the reduction of cuprous oxides in absence of chloride [28,31]. This plateau is thus attributed to the following reaction:



The open circuit potential is actually located in the domain where cuprous species are stable.

- The second potential plateau appeared when the copper electrode was left in chloride medium, thus this plateau can be allocated to the reduction of cuprous chloride.



When films are formed in the presence of PDTC, the current plateaux corresponding to Cu_2O and CuCl reduction are in some cases badly separated. Besides, except for the electrode immersed in $10^{-4} \text{ mol L}^{-1}$ PDTC, the plateau potentials were shifted towards more negative values for both immersion times.

Table 2 recapitulates the values of the plateaux potentials and their corresponding charges. In this table, the plateau potential was determined when one half of the corresponding species was reduced. It can be seen that this potential shifts towards more negative value for both plateaux when a higher PDTC content was added, and also for the longer immersion period. The PDTC stabilized therefore the surface species, both CuCl and Cu_2O , making the reduction reaction more difficult hence increases the overpotential for the reduction.

In terms of electrical charges corresponding to the species reduction, it can be seen from this table that the total charge involved after 1 hour immersion showed no clear tendency. In contrast, after 24 hours immersion, the total charge decreased significantly, essentially due to the first potential arrest plateau corresponding to Cu_2O reduction. Indeed, without or with $10^{-4} \text{ mol L}^{-1}$ of PDTC, Cu_2O amount increases significantly compared to that of CuCl , particularly for 24 hours of immersion. Moreover, the amount of Cu_2O is lower in the layers formed on copper in $10^{-3} \text{ mol L}^{-1}$ or $10^{-2} \text{ mol L}^{-1}$ of PDTC. For these high concentrations, PDTC is involved in Cu_2O formation making this film more stable and slowing down copper oxidation.

Further exploitation of these results allows calculating the mass accumulated on the copper surface from the electrical charge. The quantities of O and Cl contributing to the formation of Cu₂O and CuCl were then respectively determined from the charges of the first and the second plateaux. The results are shown in Table 3.

From this table, it can be seen that after 1 hour immersion, no clear effect of PDTC can be seen especially for 10⁻³ and 10⁻² mol L⁻¹, which is in agreement with EQCM results. Indeed, as can be seen from the insert of figure 2, for the higher concentrations and after 1h immersion, films are still growing and have not yet reached their final state. On the contrary, after 24 hour immersion, the higher the PDTC concentration is, the smaller are both corrosion products (Cu₂O and CuCl) accumulated on the copper surface with some exception.

3.4 Combination of EQCM and coulometric results

It is obvious that coulometric measurements allow evaluating only the quantities of products accumulated on copper surface, and therefore do not enable determining the corrosion rate of copper with or without PDTC. On the other hand, EQCM experiments showed a mass loss in a low PDTC concentration and the mass gain when its concentration is greater than 10⁻³ mol L⁻¹. However, corrosion products form on copper even without or with low content of PDTC. By EQCM measurements, the masse loss (dissolution of copper) and the mass gain (formation of Cu₂O and CuCl) are not separated. Thus, the combination of these two techniques may allow us to calculate the corrosion rate of copper at each concentration of PDTC. This approach, to our best knowledge, is the first case where EQCM and galvanostatic reduction are coupled to evaluate the corrosion current density.

The EQCM data can be split into three contributions:

$$\Delta m_{\text{EQCM}} = \Delta m_{\text{Cu}} + \Delta m_{\text{O}} + \Delta m_{\text{Cl}} \quad (5)$$

where Δm_{Cu} , Δm_{O} , and Δm_{Cl} represent respectively the mass change induced by the dissolution of the copper (thus negative), the mass of oxygen by Cu_2O and that by CuCl . The coulometric measurements allowed evaluating $\Delta m_{\text{coulom}} = \Delta m_{\text{O}} + \Delta m_{\text{Cl}}$ accumulated at the copper surface. Consequently, the mass loss due to the copper dissolution alone can be calculated by the following equation:

$$\Delta m_{\text{Cu}} = \Delta m_{\text{EQCM}} - \Delta m_{\text{coulom}} \quad (6)$$

Δm_{EQCM} is determined on Fig. 2 and Δm_{coulom} displayed in Table 3 as “*m total*”. Table 4 displays the copper mass loss and the corrosion current density $\langle j_{\text{corr}} \rangle$ calculated by applying the Faraday law with Cu. $\langle j_{\text{corr}} \rangle$ represents the mean value for 1 or 24 hours immersion and may then decrease progressively with time. The values obtained are thus overestimated. Besides, for low PDTC concentrations, the corrosion current density is positive and this approach supplies rather good results. However, negative $\langle j_{\text{corr}} \rangle$ was obtained in high PDTC concentrations, in total contradiction to the corrosion process. This contradictory result can be explained by four manners:

- As mentioned above, the SEM pictures showed the presence of PDTC crystals, thus the EQCM experiments overestimate the amount of corrosion products at the copper surface.
- Two coppers used were slightly different in nature, thus the corrosion rate might be different between two measurements.
- The reproducibility of the experimental results is far from ideal, and thus some discrepancy is expected in these data.
- More likely, at high concentrations of PDTC, the whole surface products were not reduced entirely when the electrode potential reached the hydrogen evolution reaction domain because PDTC makes the surface species highly stable. Evaluation of the surface species accumulated on the copper surface seemed then to be too small leading to the mass gain of copper and therefore a negative value of $\langle j_{\text{corr}} \rangle$.

All these reasons may explain the fact that despite of the combination of EQCM and coulometric measurements, $\langle j_{\text{corr}} \rangle$ values are not entirely reliable. However, globally, it is important to remark that the corrosion current density thus estimated decreased with time, that is, the inhibitive effect settled slowly with time.

3.5 Voltammetries

Two approaches were used by voltammetry to characterise the effect of PDTC on the corrosion of copper; a wide potential scan where its effect on the electrode kinetics can be visualised readily and a narrow potential scan to evaluate the corrosion current density j_{corr} by Stern – Geary relationship [32].

3.5.1 Wide potential scan

Fig. 6 presents the polarisation curves obtained in presence of PDTC at different concentrations in 0.5 mol L^{-1} NaCl after immersion for 1 or 24 hours. The anodic and cathodic characteristics were collected by independent cathodic and anodic scan experiments as mentioned above.

Except for $10^{-4} \text{ mol L}^{-1}$ PDTC, for both anodic and cathodic branches, the higher the concentration of the inhibitor is, the smaller is the current density in the whole potential domain.

3.5.1.1 Cathodic reactions:

At high overpotentials, beyond -1.2 V , the current density decreased in absolute value, that is the reduction process is hindered in the presence of PDTC.

For less cathodic potentials, several observations can be made:

- The two current peaks can be guessed one around -0.5 V and another at -0.8 V . They may correspond to Cu_2O and CuCl reduction respectively according to coulometric

measurements. The difference is that the products are reduced, here, by cathodic potential sweep.

- These current peaks shift towards more negative direction when PDTC concentration increased because surface products are stabilized by PDTC and thus a higher overvoltage is necessary for their reduction.
- These peaks move also towards more negative direction when the immersion period increased. It is also important to remark that the charge involved in cathodic peaks is the greatest at the PDTC concentration equal to 10^{-4} mol L⁻¹. Then it decreased significantly in the presence of this inhibitor.
- The current peaks were higher when the immersion period increased.

All of these changes are in agreement with the coulometric curves observed by the cathodic reduction of corrosion species. These observations show then that PDTC inhibit ORR on Cu in 0.5 mol L⁻¹ NaCl and may explain our previous preliminary inhibition tests with PDTC on Al 2024 in 0.2 g L⁻¹ NaCl [23]. It is important to recall that no inhibitive effect of PDTC was observed on pure Al, therefore it can be concluded that PDTC interacts with Cu-rich particles to hinder ORR, and consequently the corrosion rate of the aluminium alloy.

3.5.1.2 Anodic reactions:

- In the blank solution or by addition of 10^{-4} mol L⁻¹ of PDTC, the current densities tend to a plateau at high overpotential corresponding to the reaction rate determined by a diffusion process. The anodic current peak at about 0 V could be noted for these two mediums. For the highest concentration examined, however, this peak disappears completely, and a current plateau similar to passive behaviour was observed.
- The concentration at 10^{-3} mol L⁻¹ for one hour immersion constituted a transition state. From one experiment to another, two behaviours were recorded: either the appearance of

current peak at about 0 V or its disappearance similar to the polarization curves obtained at 10^{-2} mol L⁻¹. For the former, the corrosion potential E_{corr} (open circuit one) is located more positive value than for the latter. Besides, it was remarked that for the former, the cathodic current density near E_{corr} was higher and depicted a marked cathodic current peak, indicating the formation of greater corrosion products. Fig. 7 illustrates this situation. From the data shown in this figure, one can estimate that E_{corr} differed by about 0.13 V and j_{corr} changed more than ten times from experiment to experiment. The polarisation curve drawn in Fig. 6a corresponds to the case where E_{corr} is more positive thus exhibiting the anodic current peak.

The interface behaviour observed with 10^{-3} mol L⁻¹ PDTC suggests that the film formed after 1 hour immersion is not always protective. Thus, one hour is a transition time for the formation of a barrier film which corroborates the results obtained by EQCM. A higher concentration, or a longer immersion time are then required to form a protective layer. When these conditions are met a large passivity-like plateau approaching, in some cases, 1 V width is obtained with low current densities. Since the open circuit potential did not change substantially, this behaviour can be explained by a marked barrier property of the surface film formed by corrosion products. This formation of barrier film can be exploited when copper is used in oxidizing conditions.

The results obtained in this section show that PDTC decreases, when added sufficiently, the current densities of both anodic and cathodic reactions. Therefore, this inhibitor will be considered as a mixed inhibitor.

3.5.2 Narrow potential scan

Polarization curves of narrow potential range were performed on copper for different concentrations of PDTC (Fig. 8). The sample was left in the solution during 1h or 24h and

then the polarization curve was plotted ± 30 mV with respect to the open circuit potential, from cathodic to anodic potentials.

The corrosion current density can be evaluated by applying the Stern – Geary relationship [32]. The regression calculation using non-linear least-square method was applied to evaluate the corrosion parameters: j , j_{corr} , E_{corr} , b_a and b_c that are respectively the experimentally observable current density, corrosion current density, corrosion potential where the overall current is zero, the Tafel coefficient of anodic and cathodic process. The results are summarized in Table 5. Calculated polarization curves were overlaid by solid lines on experimental data presented by symbols. It can be seen that the Stern – Geary relationship suitably represents the experimental polarization curves.

The higher the inhibitor concentration is, the smaller is the corrosion current density as well for the short as for the long immersion period. For a given inhibitor concentration, the corrosion rate decreased with the immersion period, thus, as stated above, the corrosion products covering the electrode surface protect the substrate copper. b_a values decreased when the PDTC concentration increased as can be readily evaluated from the wide range polarization curves. b_c , though scattered considerably, no clear tendency can be seen from these data. The value of the Stern – Geary coefficient B that links the corrosion rate and the slope of the polarization curves (R_p), $B = 1/(b_a-b_c)$ does not change significantly. Thus the mean B value of these data can be used to evaluate the corrosion rate (section 3.7) from the polarization resistance measurements R_p (determined from EIS tests) with the following relationship [32]:

$$j_{\text{corr}} = \frac{B}{R_p} = \frac{0.024}{R_p} \quad (7)$$

3.6 Electrochemical Impedance Spectroscopy

EIS measurements were carried out during 48 hours, and the impedance data were collected every hour. As for an example, Fig. 9 presents the impedance spectrum obtained after 3 hours immersion in the presence of 10^{-3} mol L⁻¹ PDTC. Though it is difficult to see the presence of a capacitive loop in high frequency domain in the Nyquist plot (Fig. 9a), the Bode plot (Fig. 9b) shows clearly the presence of a high frequency capacitive loop above several kHz. The impedance spectra obtained involves therefore three time constants.

Though the time constants are not always clearly separated as illustrated here, especially in an early immersion period in the blank test solution, all experimental spectra contained three time constants, typical for the copper or copper alloy electrode in a mildly aggressive medium in the presence of a CuCl or a patina layer [24, 33-34]. Therefore, the electrical equivalent circuit illustrated in Fig. 10 was used for the parameter regression calculation using a Simplex method. This remark suggests that the addition of PDTC in the corrosion test solution does not alter the structure of the electrode surface but modifies its reactivity or the barrier property of the surface film in agreement with the polarization curves obtained with wide potential scan.

The physical nature of these elements is as follows.

- The high frequency loop R_f - C_f :
 - R_f : Film resistance representing the ionic leakage through the surface film.
 - C_f : Film capacitance due to the dielectric nature of the surface film.
- The medium frequency loop R_t - C_d :
 - R_t : Charge transfer resistance describing the sum of all charge transfer processes taking place at the electrode interface.
 - C_d : Double layer capacitance at the electronic conducting and ionic conducting interface.

- The low frequency loop R_F-C_F :
 - R_F : Faradaic resistance associated specifically with the rate of oxidation-reduction process which constitutes the difference with R_t .
 - C_F : Faradaic capacitance due to the oxidation-reduction process. Corrosion products accumulated at the electrode surface play as reservoir of the electrical charge.
- n_f, n_d, n_F : Cole-Cole coefficients representing the depressed feature of the capacitive loops in Nyquist diagrams [35-36].

This depressed shape was expressed by the equation identical to the Cole-Cole frequency dispersion of dielectrics:

$$Z = \frac{R}{1 + (j \cdot \omega \cdot R \cdot C)^n} \quad (8)$$

Figs 11, 12, and 13 present respectively for the highest, the medium and the lowest frequency capacitive loops, the results of a regression calculation with an in-house Simplex program based on the down-hill algorithm [37].

3.6.1 $R_f - C_f$ couple

In previous work on the patinated and bare Cu-Sn bronze, it was concluded that the film resistance is closely related to the patina layer and not to the cuprite (Cu_2O) layer [34,38]. Thus, it is very likely that this resistance is to be associated with CuCl layer, and its barrier effect was reinforced by PDTC.

Note that R_f increased with increasing PDTC concentration except for 10^{-4} mol L⁻¹ PDTC for a short immersion period. After 48 hours immersion in the solution containing 10^{-2} mol L⁻¹ PDTC, R_f reached 386 kΩ cm² whereas R_f for the blank solution reached only 9.81 Ω cm². On the contrary, the addition of 10^{-4} mol L⁻¹ PDTC increased this resistance only

slightly. This observation is in agreement with a poor protective property of surface film when PDTC concentration is low as stated above (c.f. §3.2.).

The film capacitance C_f , decreased when the PDTC concentration increased, indicating thickening of the surface film (cf. Table 6). It is important to note that changes in R_f and C_f were slower in the presence of 10^{-3} mol L⁻¹ PDTC than those observed with 10^{-2} mol L⁻¹ in agreement with EQCM and coulometric measurements though for the former experiments the mass change was induced both by Cu₂O and CuCl layer formation (cf. Table 3) whereas the $R_f - C_f$ is associated to CuCl layer alone. Hence, by combining the results obtained by EQCM, coulometry, and EIS, one can assume that the stabilization of corrosion products by PDTC is more significant on CuCl film and seems to take more time at 10^{-3} mol L⁻¹. By using the planar condenser model, the film thickness d was evaluated by the following equation:

$$d = \frac{\varepsilon \cdot \varepsilon_0}{C_f} \quad (9)$$

Here, ε and ε_0 stand respectively for the relative dielectric constant and the dielectric constant of vacuum. The value of ε , was considered to be equal to 7.5 [39].

As for the comparison, the film thickness calculated from the coulometric measurements of the second plateau by galvanostatic reduction, i.e. the charge necessary to reduce the CuCl layer (cf. Table 3 indicated as the mass of Cl at the surface) is also presented in Table 6.

$$d(Q_2) = \frac{m}{\rho} \cdot \frac{M_{\text{CuCl}}}{M_{\text{Cl}}} \quad (10)$$

Where ρ represents the specific density of CuCl (4.15 g mL⁻¹), m being the masse of Cl calculated from coulometric measurements ($\mu\text{g cm}^{-2}$, table 3), and M_{CuCl} and M_{Cl} denote respectively the molecular mass of CuCl and Cl respectively.

Note that the film thickness evaluated from C_f is thinner than that estimated from the coulometric measurements for the blank and 0.1 mM PDTC whereas the opposite trend is

observed for 1 and 10 mM. According to the thickness calculated from EIS measurement, it increased with PDTC concentration and immersion time. On the contrary, the coulometric measurements showed its thinning of the CuCl layer. This divergence can be explained, as it was the case for sulphate patina formed on Cu-Sn bronze [34], only the inner part of the salt layer exhibits the insulating dielectric property. This inner dielectric layer, only a few molecular layers at the initial stage without inhibitor becomes thicker with the increase of PDTC concentration and also with the immersion time. Over this layer, a thick and coarse CuCl layer was likely formed by the corrosion process. In other words, by EIS measurements, C_f takes into account the thickening of CuCl by PDTC exhibiting the barrier property. On the contrary, the thicknesses evaluated by coulometric measurements correspond to CuCl layer that can be reduced cathodically which becomes thinner with the increase of PDTC concentration. On the other hand, the thinning of CuCl observed by coulometric tests could be explained, as postulated above, by the fact that in presence of high concentration of PDTC, the reduction of CuCl layer is not complete when the hydrogen reduction reaction starts to take place.

Note also that between the blank and 10^{-2} mol L⁻¹ PDTC solution, the thickness of the dielectric layer estimated from C_f increases by about 50 and 10 times respectively for 1 and 24 hours immersion, whereas the R_f increased by three or four orders of magnitude. That is, the resistivity of the inner compact layer increased substantially in presence of PDTC.

3.6.2 $R_t - C_d$ couple

As can be seen in Fig. 12a, the charge transfer resistance R_t increased with immersion time. In addition, R_t increased with the PDTC concentration except for the 10^{-4} mol L⁻¹ PDTC solution where no significant difference was observed as compared to the blank test. At the 48th hour immersion time, R_t was 20 times greater at the concentration of 10^{-3} and 100 times as great at

10^{-2} mol L⁻¹ PDTC compared with the blank test. Therefore, the adsorption of PDTC at the Cu surface hinders strongly its electro-reactivity in NaCl medium.

C_d in 10^{-2} M PDTC decreased very quickly from the initial time indicating that the adsorption of PDTC at the copper surface was rather fast, whereas R_t increased slowly. The same behaviour, less pronounced, is observed at 10^{-3} M PDTC. Thus, the inhibitive effect of PDTC to the reaction rate evolved more slowly with immersion period. At the concentration of 10^{-2} mol L⁻¹ PDTC and at the 48th hour of immersion, C_d decreased by more than 2000 times, thus the surface area where the electrolyte was in contact with electronic conducting species becomes very small.

3.6.3 $R_F - C_F$ couple

This couple was attributed mainly to the kinetics of the reversible redox process between Cu and Cu₂O (Eq. 3) as can be deduced from Table 2, and Fig. 5 showing the amount of Cu₂O much higher compared with CuCl. It should be noticed also that the redox potential of Cu \leftrightarrow Cu₂O is much less negative than that of Cu \leftrightarrow CuCl and therefore, the reversible redox process should be more closely associated with Cu / Cu₂O. In spite of the increase of the Cu₂O amount with immersion period, C_F decreased. This indicated that the active reactivity of Cu₂O taking part in the redox process decreased with time.

R_F at 10^{-2} mol L⁻¹ PDTC increased very quickly with immersion time in agreement with the change in C_d . The adsorption of PDTC likely decreased the redox reaction rate between Cu and Cu₂O.

The EIS data allowed us to summarize the effect of PDTC as follows: The formation of CuCl - PDTC complex improves its ionic barrier property according to R_f change. In parallel, as attested by R_t change, PDTC will be adsorbed directly on Cu surface making its corrosion resistance higher. Besides, PDTC make lower the electrochemical reactivity of Cu₂O layer.

3.6.4 Polarization resistance R_p

It was shown that in the presence of redox processes, the polarization resistance, and not the charge transfer resistance, is the most closely correlated with the corrosion rate [34,40]. Since R_f is non-faradaic entity, the polarization resistance is defined as:

$$R_p = R_t + R_F \quad (11)$$

Fig. 14 presents the variation of R_p with respect to the immersion time in the presence of different concentrations of PDTC. It can be seen that R_p increased with immersion time and also with PDTC concentrations as expected from the results presented above. Up to 24 hours immersion, 10^{-4} mol L⁻¹ PDTC has little inhibitive effect, but beyond this period, its protective effect appears. More precisely, this improvement takes place beyond 12 hours as we have seen through EQCM results (Fig 2) and the inhibiting efficiency reached 91 % at 48 hours immersion. At a PDTC concentration equal to 10^{-2} mol L⁻¹, the inhibitive effect reached 99.8 % after 2 days immersion.

3.7 Comparison of the inhibitive effect evaluated with different methods

Various methods were applied as described above to evaluate the inhibitive effect of PDTC to the corrosion of copper in 0.5 mol L⁻¹ NaCl solution in the presence of various concentration of PDTC. Table 7 summarizes the inhibitive efficiency calculated from different experimental methods employed in this study. For the blank test solution, the corrosion current density, instead of the inhibiting efficiency, as determined by these techniques is displayed.

By taking into account of the corrosion current density in presence of PDTC also, not presented here, it was remarked that the EQCM technique did not allowed the correct estimation of the corrosion rate j_{corr} . The corrosion current densities were generally too small due to the over simplification of the hypotheses used. By combining EQCM and coulometric results, the corrosion current density was calculated rather correctly in absence of the

inhibitor. However, the copper mass change ($\Delta m(\text{Cu})$, table 4) was sometimes evaluated as positive, since as assumed in section coulometry, corrosion products were not completely reduced probably because of their stabilization by PDTC. The positive mass loss leads to the calculated inhibitive efficiency greater than 100. The voltammetry and EIS supply consistent data. The protective efficiency is estimated to be greater than 99 % when $10^{-2} \text{ mol L}^{-1}$ PDTC was added in 0.5 mol L^{-1} NaCl solution.

4. Conclusions

This work was devoted to study the electrochemical behaviour of Cu / 0.5 mol L^{-1} + PDTC system to understand the interaction between PDTC and Cu-rich particles contained in some aluminium alloys. By combining different electrochemical methods, relevant results were obtained:

- PDTC is a good mixed inhibitor for Cu in 0.5 mol L^{-1} NaCl. PDTC acts by stabilizing the surface products that are formed on copper in chloride media i.e. CuCl and Cu₂O. This stabilization is so strong that these products were not completely reduced under cathodic current.
- At $10^{-4} \text{ mol L}^{-1}$, PDTC was found in the corrosion products (cf. Section 3.2) but this concentration is not sufficient to stabilize the products. However a slight decrease in the corrosion rate was observed after 12 h of immersion.
- At high concentrations, PDTC reduces considerably the copper surface area exposed to aggressive species and then hinders strongly the reactivity of the electrode, leading to high inhibitive efficiencies. This is more pronounced at $10^{-2} \text{ mol L}^{-1}$.
- A quaint result was observed for the anodic behaviour of the copper at $10^{-3} \text{ mol L}^{-1}$ PDTC showing that 1 h immersion seems to be a transition time to stabilize the corrosion products at this concentration.

These findings are highly useful for various applications of copper. Moreover, regarding our main objective and as shown in Fig. 6, the cathodic current density decreased dramatically in presence of sufficient concentration of PDTTC. This compound decreases then the rate of ORR on pure copper. As ORR takes place on copper rich particles in 2xxx series aluminium alloys, this finding explains some results obtained with preliminary tests on Al 2024 [23]. This is encouraging for further investigations.

Acknowledgements

The University of El Jadida who authorized Pr. W. Qafsaoui to attend the LISE before the end of University year is gratefully acknowledged.

References

1. P. Schmutz, G.S. Frankel, *J. Electrochem. Soc.* 145 (1998) 2295.
2. W. Zhang, G.S. Frankel, *Electrochim. Acta*, 48 (2003) 1193.
3. Military Specification MIL-C-81706, Chemical Conversion Materials for Coating Aluminum and Aluminum Alloys, June 1970.
4. W. Qafsaoui, H. Huet, H. Takenouti, *J. Electrochem. Soc.*, 156, (2009) C67.
5. W. Qafsaoui, H. Takenouti, *Corros. Sci.* 52 (2010) 3667.
6. Y. I. Kuznetsov, *Organic Inhibitors of Corrosion of Metals*, Plenum Press, New York, NY, 1996.
7. N. K. Patel, J. Franco, I. S. Patel, *J. Ind. Chem. Soc.* 54 (1997) 815.
8. C. W. Yan, H. C. Lin, C. N. Cao, *Electrochim. Acta* 45 (2000) 2815.
9. F. Ammelot, C. Fiaud, E. M. M. Sutter, *Electrochim. Acta* 42 (1997) 3565.
10. K. Aramaki, T. Kiuchi, T. Sumiyoshi, H. Nishishara, *Corros. Sci.* 32 (1991) 593.

11. G. Xue, J. Ding, P. Lu, J. Dong, *J. Phys. Chem.* 95 (1991) 7380.
12. J. Bukowska, A. Kudelski, *J. Electroanal. Chem.* 309 (1991) 251.
13. R. Yonda, H. Nishishara, K. Aramaki, *Corros. Sci.* 28 (1988) 87.
14. D. Tromans, R. Sun, *J. Electrochem. Soc.* 138 (1991) 3235.
15. G. Williams, A. J. Coleman, H. N. MacMurray, *Electrochim. Acta* 55 (2010) 5947.
16. M. Kendig, Melitta Hon, John Sinko, *ECS Trans.*, 1 (2006) 119.
17. M. Kendig, M. Hon, *Electrochem. Solid-State Lett.* 8 (2005) B10.
18. M. Kendig, C. Yan, *J. Electrochem. Soc.* 151 (2004) B679.
19. J. Chen, C. Du, J. Kang, J. Wang, *Chemico-Biological Interactions*, 171 (2008) 26.
20. A. E. Al-Rawajfeh, E. M. Al-Shamaileh, *Desalination*, 206 (2007) 169.
21. Q.-Q. Liao, Z.-W. Yue, D. Yang, Z.-H. Wang, Z.-H. Li, H.-H. Ge, Y.-J. Li, *Thin Solid Films*, 519 (2011) 6492.
22. W. Qafsaoui , M. Kendig, H. Takenouti, F. Huet, 213th Meeting of the Electrochemical Society, Symposium "Corrosion General Session", Phoenix (USA), Mai 2008. Ext. Abstr. N° 609.
23. M. Kendig, W. Qafsaoui , H. Takenouti, F. Huet, Nace Research in Progress Symposium, session: Coatings and Inhibitors, Corrosion/08, New Orleans- Louisiana (USA), Mars 2008.
24. Helena Otmacic Curkovic, Ema Stupnisek-Lisac, Hisasi Takenouti, *Corros. Sci.* 52 (2010) 398.
25. G. Sauerbrey, Verwendung von Schwingquarzen zur Wägung dünner Schichten zur Mikrowägung, *Z. Phys.*, 155 (1959) 206.

26. C. Arkam, V. Bouet, C. Gabrielli, G. Maurin, H. Perrot, J. Electrochem. Soc., 141 (1994) L103.
27. Carl Roth, Safety data card : 5486f.PDF; <http://www.carlroth.com/media/fr-ch/sdpdf/5486f.PDF>.
28. W. Qafsaoui, C. Blanc, N. Pébère, H. Takenouti, A. Srhiri, G. Mankowski, Electrochim. Acta, 47 (2002) 4339.
29. H.P. Lee, K. Nobe, J. Electrochem. Soc. 133 (1986) 2035.
30. C. Deslouis, B. Tribollet, G. Mengoli, M.M. Musiani, J. Appl. Electrochem. 18 (1988) 384.
31. K. Rahmouni, M. Keddou, A. Srhiri, H. Takenouti, Corros. Sci. 47 (2005) 3249.
32. M. Stern, A.L. Geary, J. Electrochem. Soc. 104 (1957) 56.
33. K. Marušić, H. Otmačić Čurković, S. Horvat-Kurbegovic, H. Takenouti, E. Stupnišek-Lisac, Electrochim. Acta, 54 (2009) 7106.
34. K. Marušić, Helena Otmačić Čurković, Hisasi Takenouti, Electrochim. Acta 56 (2011) 7491.
35. E. Barsoukov, J.R. Macdonald, Impedance spectroscopy, Theory, experiment, and applications, pp 16-20, (2005) John Wiley and Sons, New York (NY).
36. K.S. Cole, R.H. Cole, J. Chem. Phys. 9 (1941) 341.
37. W.H. Press, B.P. Flannery, S.A. Toukolsky, W.T. Vetterling, Numerical Recipes, Cambridge University Press (1987).
38. L. Muresan, S. Varvara, E. Stupnišek-Lisac, H. Otmačić, K. Marušić, S. Horvat-Kurbegović, L. Robbiola, K. Rahmouni, H. Takenouti, Electrochim. Acta, 52 (2007) 7770.

39. C. Noguét, C. Schwab, C. Sennett, M. Sieskind, C. Viel, J. Phys. France 26 (1965) 317.
40. I. Epelboin, C. Gabrielli, M. Keddam, H. Takenouti, A-C impedance measurements applied to corrosion studies and corrosion rate determination, in "Electrochemical Corrosion Testing", F. Mansfeld, U. Bertocci editors, STP 727, 150-192. American Society for Testing and Materials, Philadelphia, Pa (1981).

Table captions

Table 1: Rate of mass change at the beginning (1-4 hours) and the end (21-24 hours) of immersion test in absence and in presence of PDTC at different concentrations.

Table 2: Potentials and charges corresponding to the plateaux obtained by reduction of corrosion products formed on Cu electrode in 0.5 mol L^{-1} NaCl in presence of different concentrations of PDTC, and then reduced in borate buffer solution purged of dissolved oxygen at $-50 \mu\text{A cm}^{-2}$.

Table 3: Quantities of O and Cl involved in Cu_2O and CuCl formation determined from the charges Q_1 and Q_2 corresponding to Cu_2O and CuCl reduction.

Table 4: Copper mass loss calculated from the EQCM and coulometric measurements at 1 and 24 hours immersion at different PDTC concentrations.

Table 5: The corrosion kinetic parameters of Cu in 0.5 mol L^{-1} NaCl in absence and in presence of PDTC at different concentrations for two different immersion times.

Table 6: Film capacitance C_f at 1 and 24 hour immersion and the estimation of the CuCl film thickness for Cu electrode immersed in 0.5 mol L^{-1} NaCl in presence of different concentrations of PDTC. $d(Q_2)$ is the thickness of CuCl film calculated from coulometric results.

Table 7: The inhibitive effect of PDTC at different concentrations determined by various techniques used in this study. For the blank test solution, the corrosion current density estimated by each method is shown.

Figure captions

Figure 1: 1-pyrrolidine dithiocarbamate ($M=147.26 \text{ g mol}^{-1}$).

Figure 2: Gravimetric measurements on electrochemically deposited Cu in presence of different concentrations of PDTC (1 pyrrolidine dithiocarbamate) in 0.5 mol L^{-1} NaCl. The insert indicates an initial mass change in enlarged scale.

Figure 3: SEM image of copper surface after 24 hours immersion in 0.5 mol L^{-1} NaCl + $10^{-4} \text{ mol L}^{-1}$ PDTC (a) and EDX analysis of the film (b).

Figure 4: SEM image of copper surface after 24 hours immersion in 0.5 mol L^{-1} NaCl + $10^{-2} \text{ mol L}^{-1}$ PDTC (a) and EDX analysis of the ridge area (b) and the crystal (c).

Figure 5: Galvanostatic reduction of surface layers formed on the Cu electrode in 0.5 mol L^{-1} NaCl in presence of PDTC at different concentrations after 1 (a) or 24 (b) hours immersion. The reduction was carried out at $-50 \mu\text{A cm}^{-2}$ in 0.01 mol L^{-1} H_3BO_3 + 0.01 mol L^{-1} $\text{Na}_2\text{B}_4\text{O}_7$ (pH 9) purged of dissolved oxygen by Ar.

Figure 6: Effect of PDTC at different concentrations on the electrode kinetics of copper electrode in 0.5 mol L^{-1} NaCl solution at $20 \text{ }^\circ\text{C}$.

Figure 7: Two different polarization curves collected after one hour immersion in presence of $10^{-3} \text{ mol L}^{-1}$ PDTC; the presence or the absence of the anodic current peak at about 0 V_{SCE} .

Figure 8: The polarization curves of narrow potential range to evaluate the corrosion parameters after 1 or 24 hours immersion in 0.5 mol L^{-1} NaCl in presence of different PDTC concentrations at $20 \text{ }^\circ\text{C}$. Stationary Cu electrode.

Figure 9: An example of the impedance spectra obtained with Cu electrode in 0.5 mol L^{-1} NaCl solution in presence of $10^{-3} \text{ mol L}^{-1}$ PDTC. Symbols (-) are experimental

data and lines with + are calculated spectrum by fitting procedure.

(a) Nyquist plot, the parameter indicated close to the Nyquist diagram is the frequency in Hz at which the impedance data was collected (b) Bode plot.

Figure 10: Electrical equivalent circuit to reproduce experimental impedance spectra for Cu electrode in NaCl solution with or without PDTC.

Figure 11: R_f and C_f (highest frequency loop) change as a function of immersion period for Cu / 0.5 mol L⁻¹ NaCl + PDTC at different concentrations; stationary electrode at 20 °C.

Figure 12: R_t and C_d (medium frequency loop) change as a function of immersion time for Cu / 0.5 mol L⁻¹ NaCl + PDTC at different concentrations; stationary electrode at 20 °C.

Figure 13: R_F and C_F (lowest frequency loop) as a function of immersion time in Cu / 0.5 mol L⁻¹ NaCl + PDTC at different concentrations; stationary electrode at 20 °C.

Figure 14: Variation of the polarization resistance R_p with respect to the immersion time. Cu / 0.5 mol L⁻¹ NaCl + PDTC at different concentrations; stationary electrode at 20 °C.

Figures

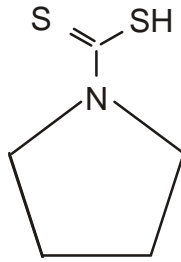


Figure 1: 1-pyrrolidine dithiocarbamate ($M=147.26 \text{ g mol}^{-1}$).

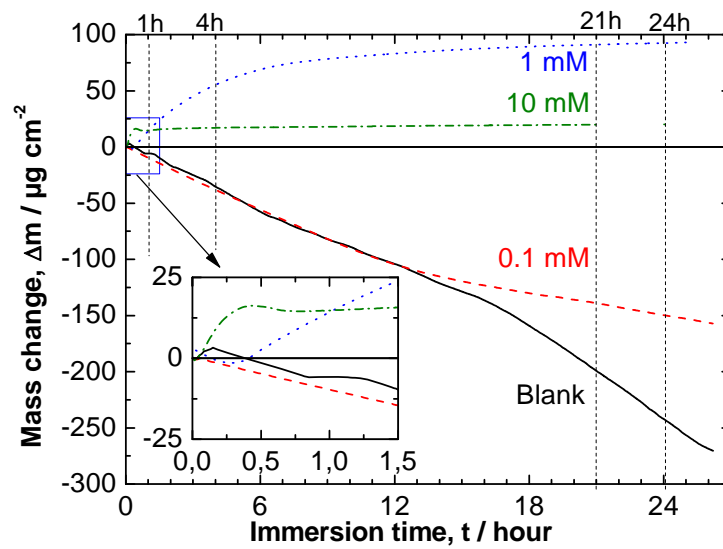


Figure 2: Gravimetric measurements on electrochemically deposited Cu in presence of different concentrations of PDTC (1 pyrrolidine dithiocarbamate) in $0.5 \text{ mol L}^{-1} \text{ NaCl}$.

The insert indicates an initial mass change in enlarged scale.

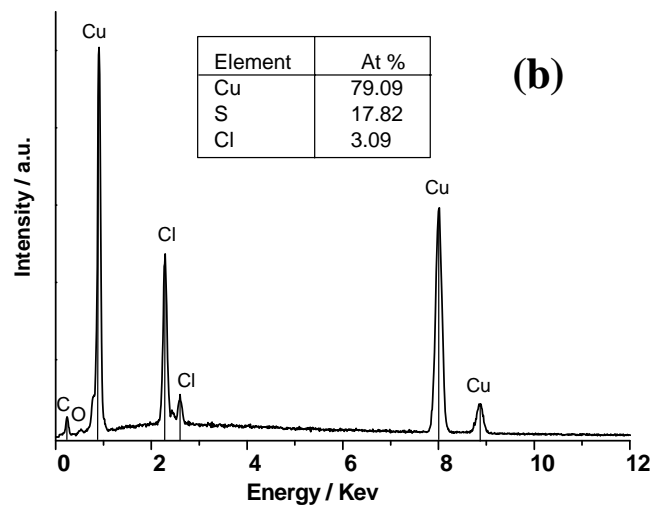
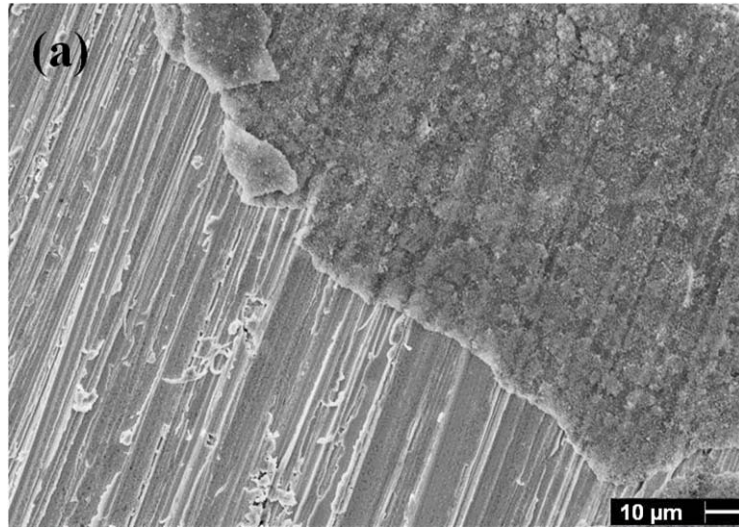


Figure 3: SEM image of copper surface after 24 hours immersion in $0.5 \text{ mol L}^{-1} \text{ NaCl} + 10^{-4} \text{ mol L}^{-1} \text{ PDTTC}$ (a) and EDX analysis of the film (b).

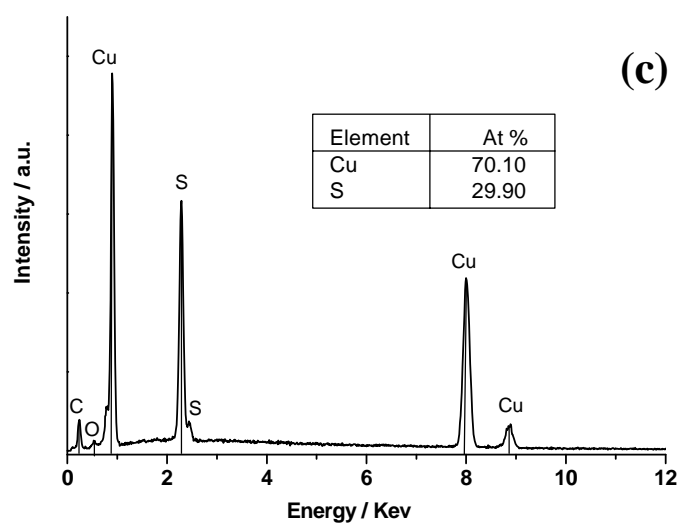
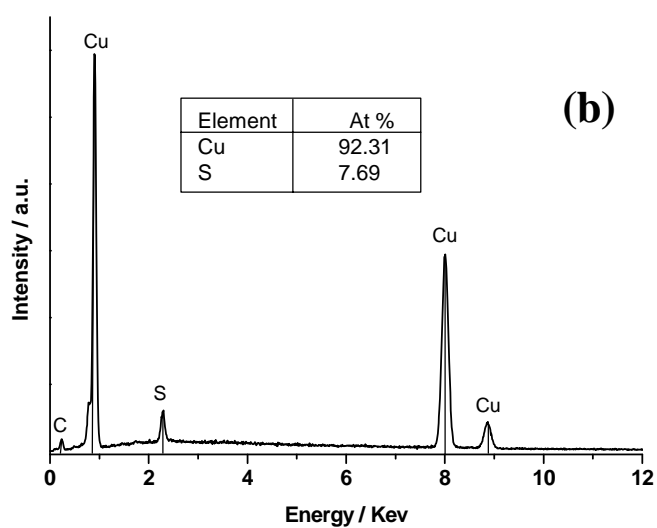
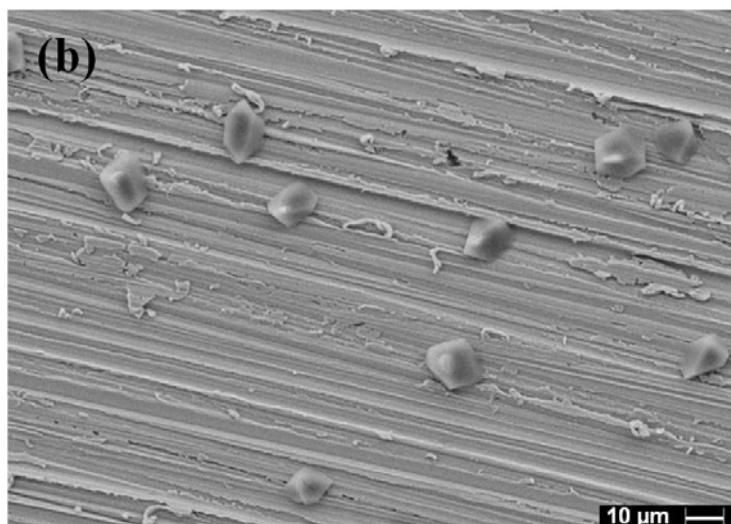


Figure 4: SEM image of copper surface after 24 hours immersion in $0.5 \text{ mol L}^{-1} \text{ NaCl} + 10^{-2} \text{ mol L}^{-1} \text{ PDTC}$ (a) and EDX analysis of the ridge area (b) and the crystal (c).

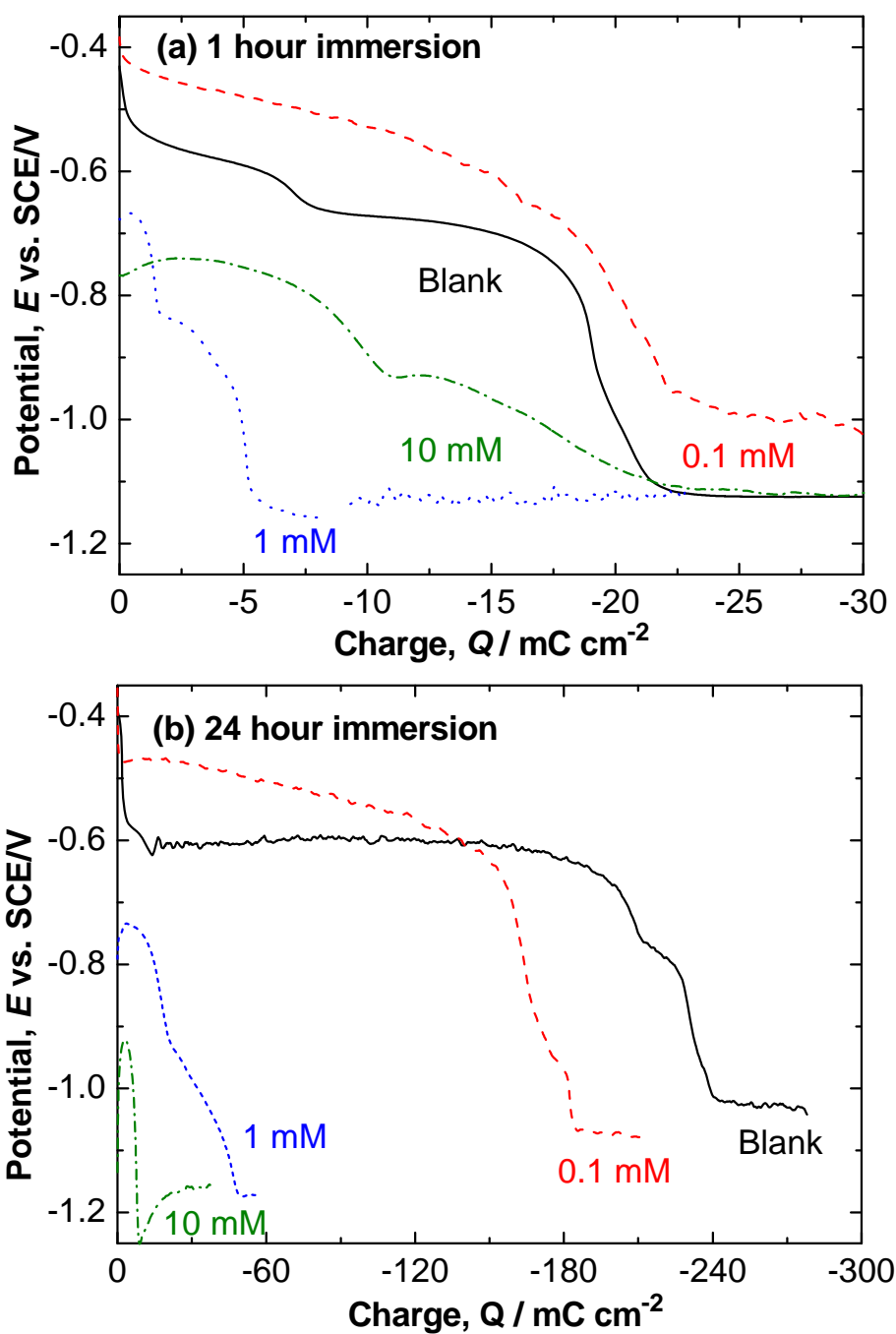


Figure 5: Galvanostatic reduction of surface layers formed on the Cu electrode in 0.5 mol L⁻¹ NaCl in presence of PDTC at different concentrations after 1 (a) or 24 (b) hours immersion. The reduction was carried out at -50 μA cm⁻² in 0.01 mol L⁻¹ H₃BO₃ + 0.01 mol L⁻¹ Na₂B₄O₇ (pH 9) purged of dissolved oxygen by Ar.

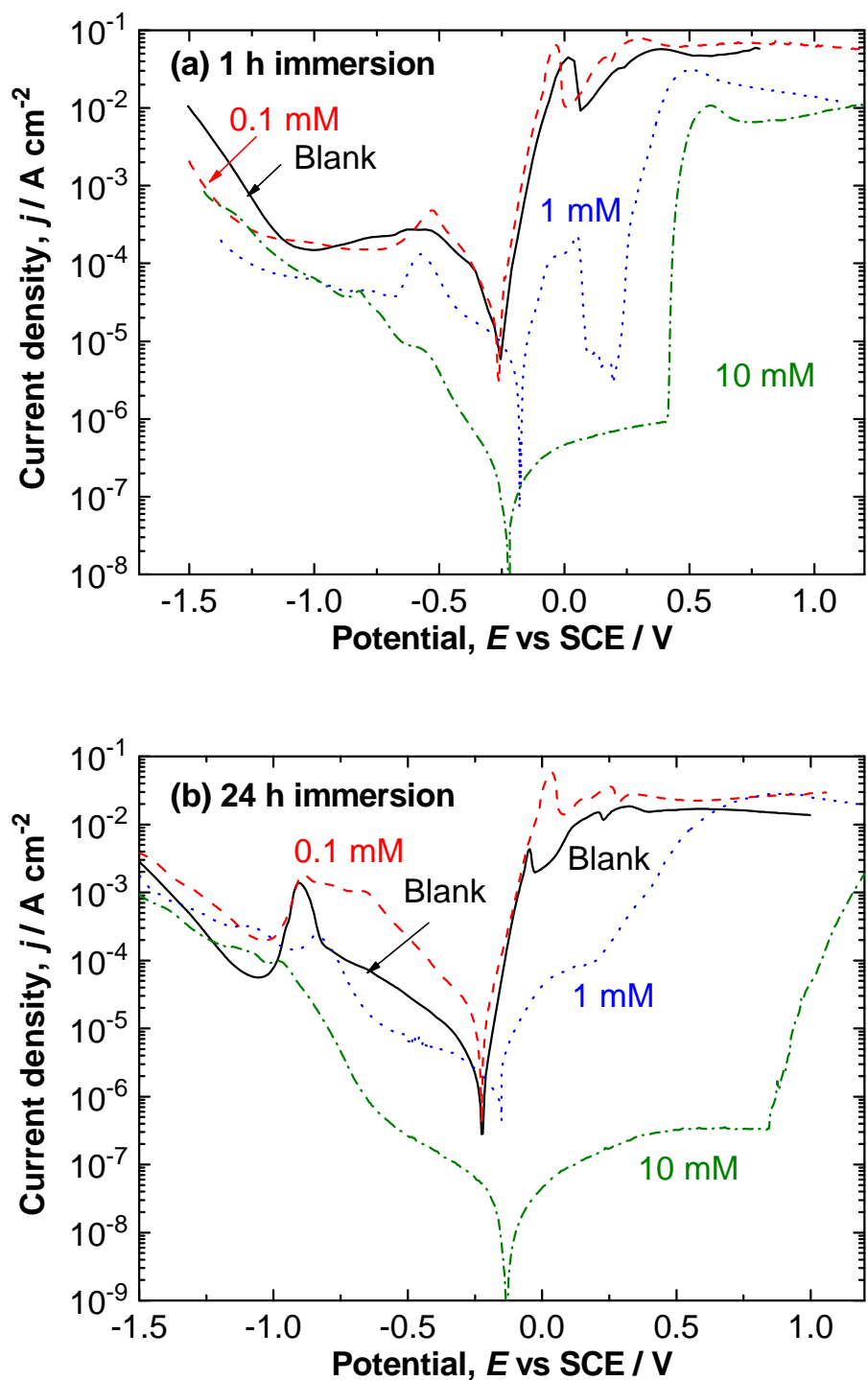


Figure 6: Effect of PDTC at different concentrations on the electrode kinetics of copper electrode in 0.5 mol L^{-1} NaCl solution at $20 \text{ }^\circ\text{C}$.

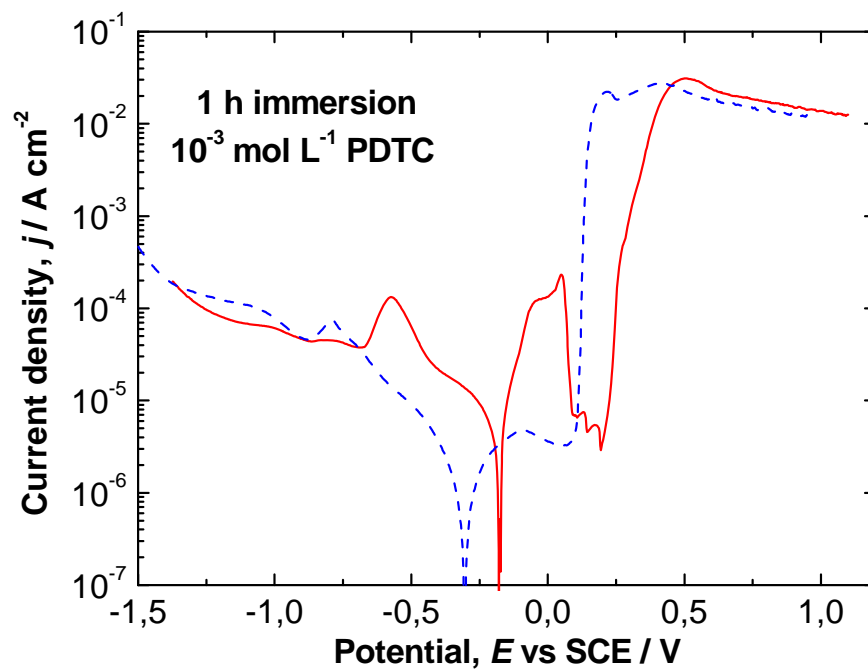


Figure 7: Two different polarization curves collected after one hour immersion in presence of $10^{-3} \text{ mol L}^{-1}$ PDTC; the presence or the absence of the anodic current peak at about 0 V_{SCE} .

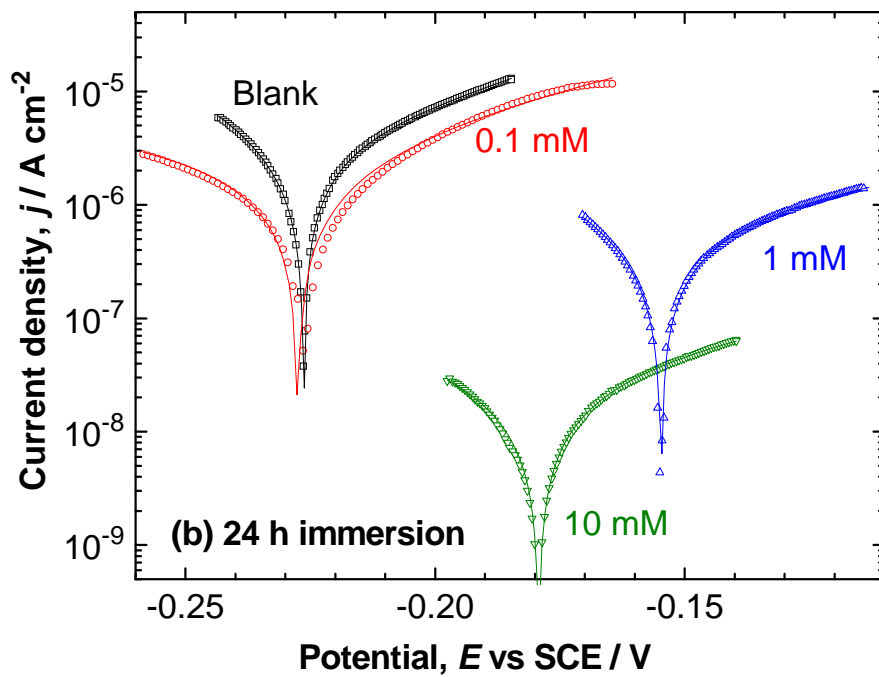
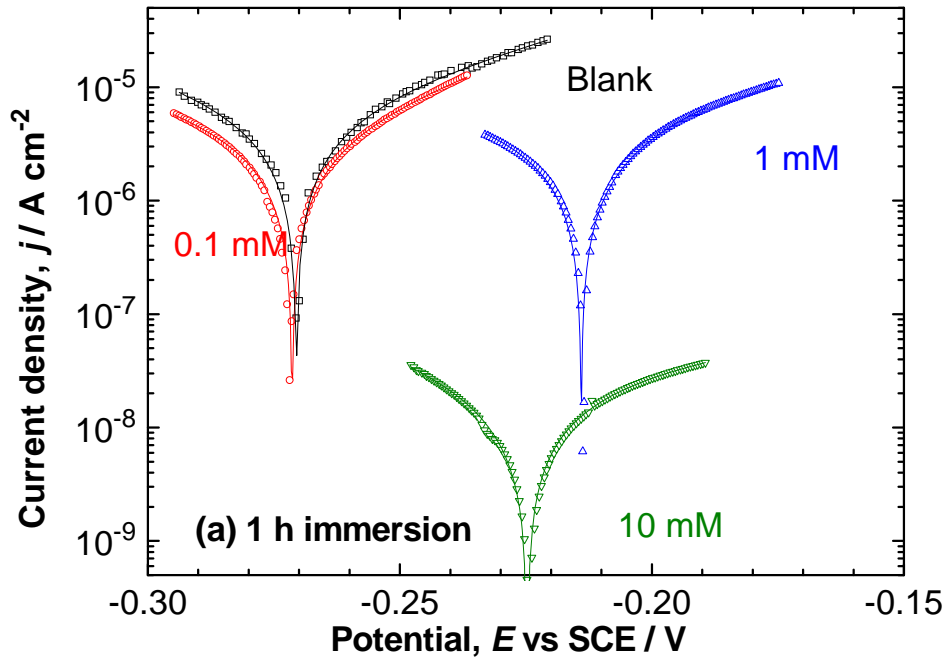


Figure 8: The polarization curves of narrow potential range to evaluate the corrosion parameters after 1 or 24 hours immersion in 0.5 mol L^{-1} NaCl in presence of different PDTC concentrations at $20 \text{ }^\circ\text{C}$. Stationary Cu electrode.

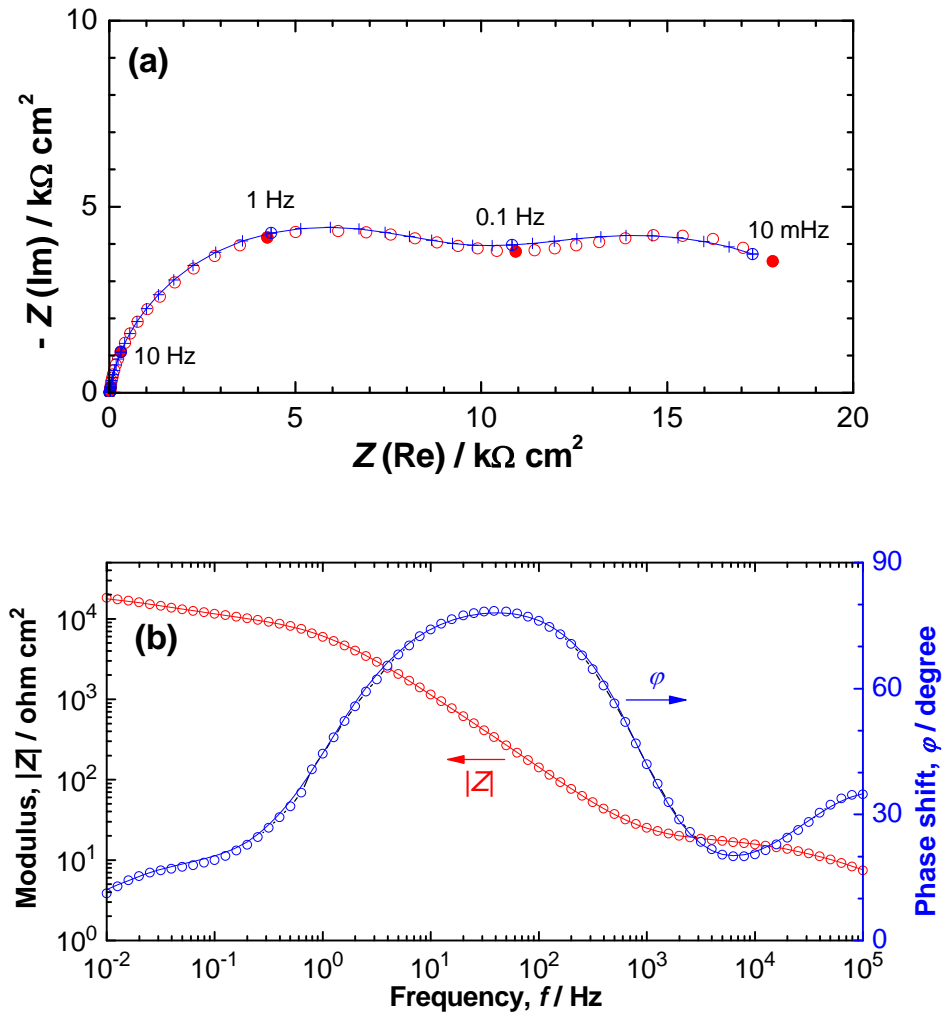


Figure 9: An example of the impedance spectra obtained with Cu electrode in 0.5 mol L^{-1} NaCl solution in presence of $10^{-3} \text{ mol L}^{-1}$ PDTC. Symbols (-) are experimental data and lines with + are calculated spectrum by fitting procedure.

(a) Nyquist plot, the parameter indicated close to the Nyquist diagram is the frequency in Hz at which the impedance data was collected (b) Bode plot.

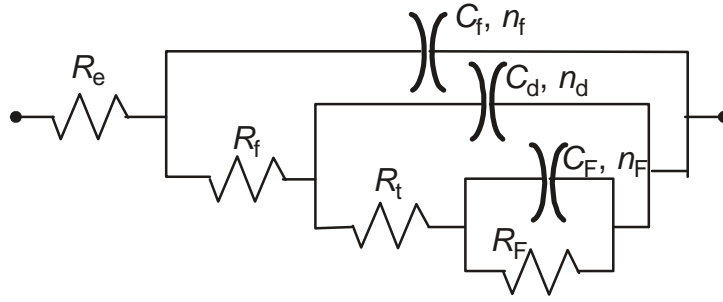


Figure 10: Electrical equivalent circuit to reproduce experimental impedance spectra for Cu electrode in NaCl solution with or without PDTC.

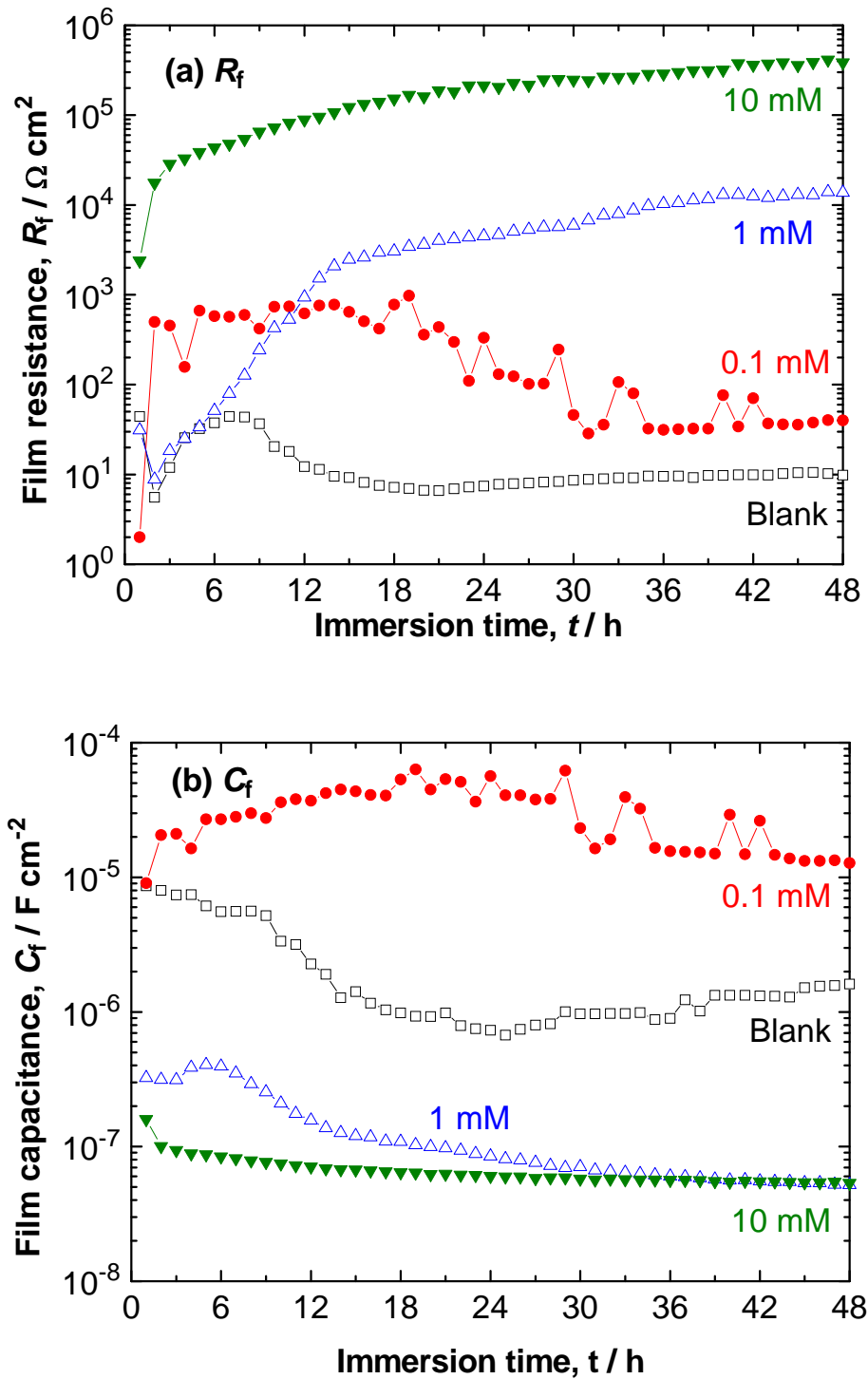


Figure 11: R_f and C_f (highest frequency loop) change as a function of immersion period for Cu / 0.5 mol L⁻¹ NaCl + PDTC at different concentrations; stationary electrode at 20 °C.

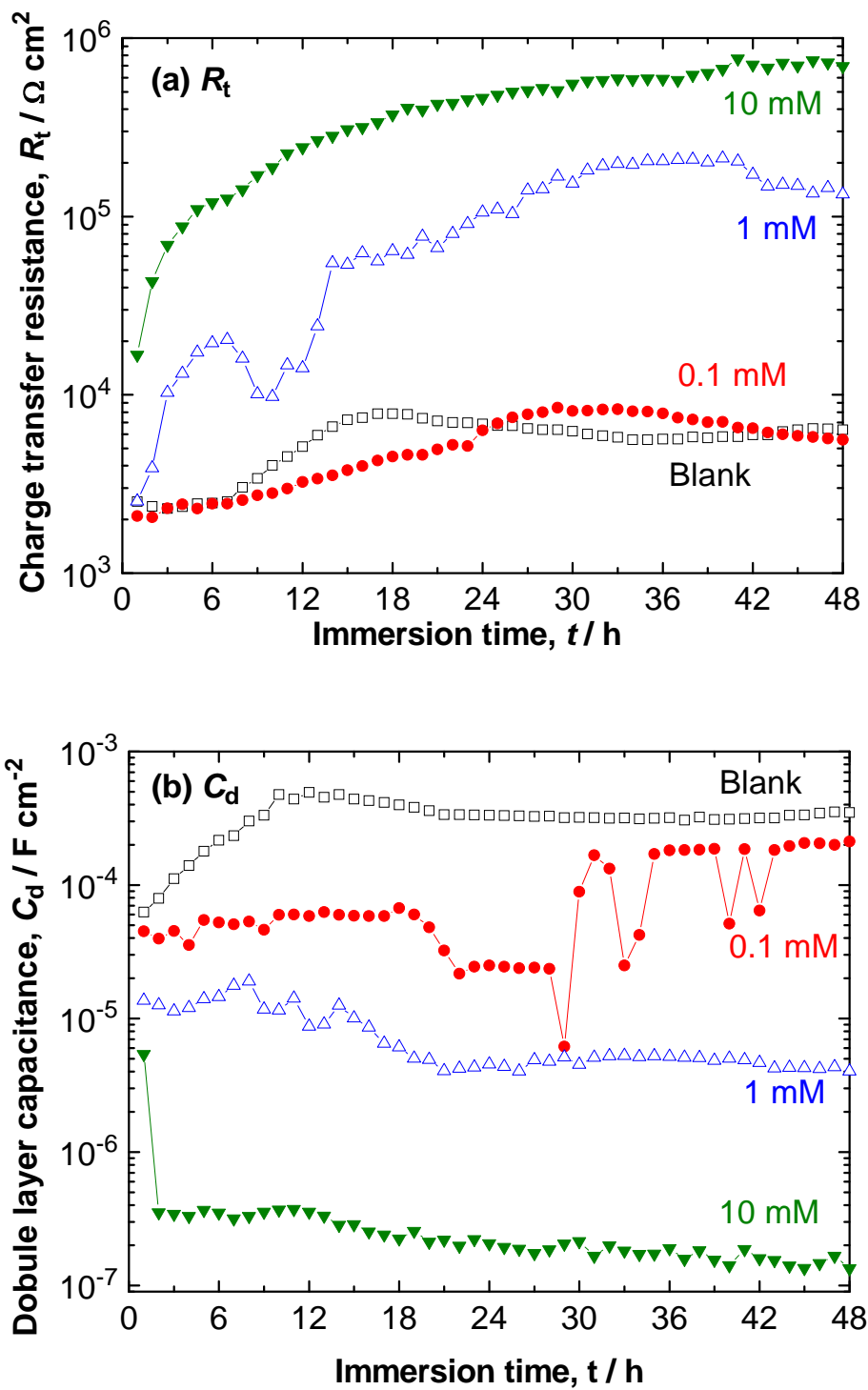


Figure 12: R_t and C_d (medium frequency loop) change as a function of immersion time for Cu / 0.5 mol L⁻¹ NaCl + PDTC at different concentrations; stationary electrode at 20 °C.

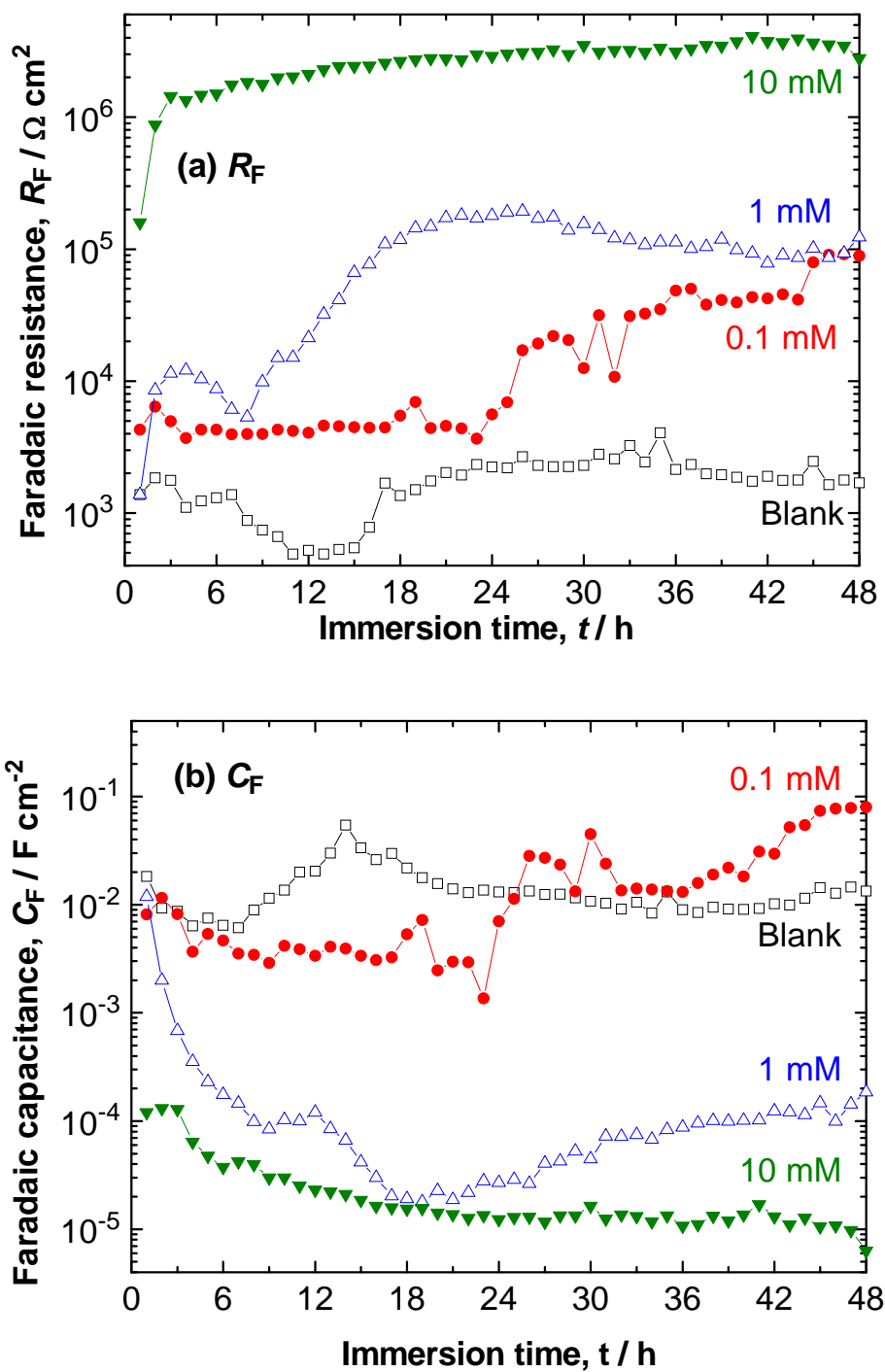


Figure 13: R_F and C_F (lowest frequency loop) as a function of immersion time in Cu / 0.5 mol L⁻¹ NaCl + PDTC at different concentrations; stationary electrode at 20 °C.

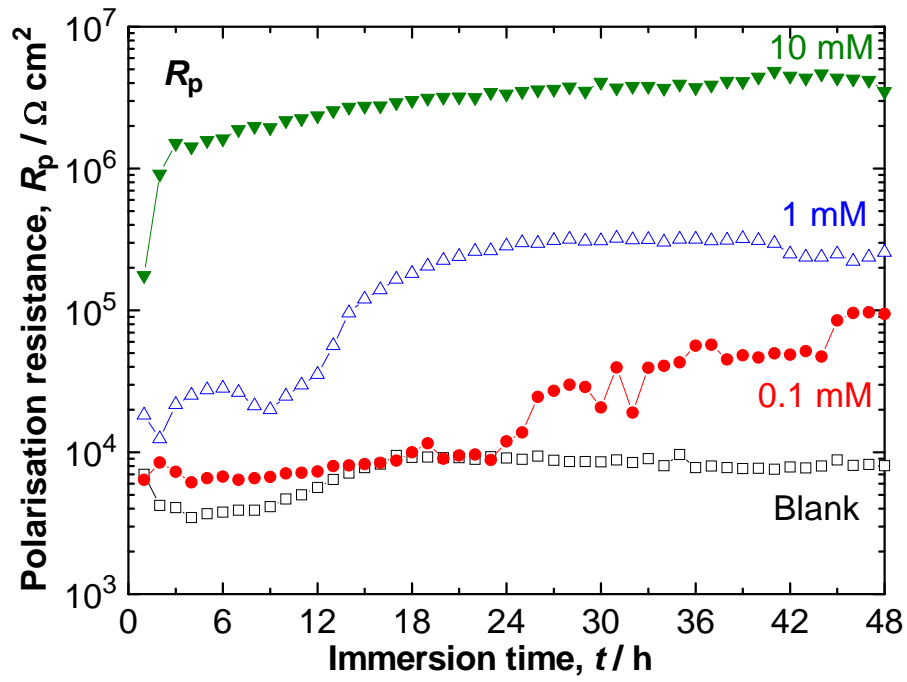


Figure 14: Variation of the polarization resistance R_p with respect to the immersion time.

Cu / 0.5 mol L^{-1} NaCl + PDTC at different concentrations; stationary electrode at $20 \text{ }^\circ\text{C}$.

Tables

Table 1: Rate of mass change at the beginning (1-4 hours) and the end (21-24 hours) of immersion test in absence and in presence of PDTC at different concentrations.

PDTC (mol L⁻¹)	1-4 h		21-24 h	
	$\Delta m/dt$ (ng s ⁻¹ cm ⁻²)	j_{corr} ($\mu\text{A cm}^{-2}$)	$\Delta m/dt$ (ng s ⁻¹ cm ⁻²)	j_{corr} ($\mu\text{A cm}^{-2}$)
0	-2.73	4.15 ^a	-4.00	6.08 ^a
10 ⁻⁴	-2.65	4.02 ^a	-0.993	1.51 ^a
10 ⁻³	3.73	10.1 ^b	0.127	0.346 ^b
10 ⁻²	0.183	0.498 ^b	0.0217	0.0591 ^b

^a Dissolution by CuCl₂⁻; ^b Formation of CuCl

Table 2: Potentials and charges corresponding to the plateaux obtained by reduction of corrosion products formed on Cu electrode in 0.5 mol L⁻¹ NaCl in presence of different concentrations of PDTC, and then reduced in borate buffer solution purged of dissolved oxygen at - 50 μA cm⁻².

<i>t</i> (hours)	PDTC (mol L ⁻¹)	First plateau (Cu ₂ O/Cu)		Second plateau (CuCl/Cu)		Total charge (Cu ⁺ /Cu)
		<i>E</i> (SCE/V)	<i>Q</i> ₁ (mC cm ⁻²)	<i>E</i> (SCE/V)	<i>Q</i> ₂ (mC cm ⁻²)	<i>Q</i> _t (mC cm ⁻²)
1	0	-0.575	-6.90	-0.679	-12.32	-18.9
	10 ⁻⁴	-0.515	-15.68	-0.676	-5.02	-20.6
	10 ⁻³	-0.673	-1.31	-0.736	-3.78	-4.99
	10 ⁻²	-0.761	-8.94	-0.937	-8.54	-17.3
24	0	-0.596	-205.5	-0.784	-26.37	-231
	10 ⁻⁴	-0.523	-162.9	-0.941	-21.13	-184
	10 ⁻³	-0.757	-17.2	-0.987	-26.16	-42.7
	10 ⁻²	-0.935	-6.28	-1.035	-3.07	-9.27

Table 3: Quantities of O and Cl involved in Cu₂O and CuCl formation determined from the charges Q₁ and Q₂ corresponding to Cu₂O and CuCl reduction.

<i>t</i> (hour)	PDTC (mol L ⁻¹)	Q ₁ (mC cm ⁻²)	<i>m</i> (O) (μg cm ⁻²)	Q ₂ (mC cm ⁻²)	<i>m</i> (Cl) (μg cm ⁻²)	<i>m</i> total (μg cm ⁻²)
1	0	-6.90	0.572	-12.32	4.53	5.10
	10 ⁻⁴	-15.7	1.30	-5.02	1.84	3.14
	10 ⁻³	-1.31	0.109	-3.78	1.39	1.50
	10 ⁻²	-8.94	0.741	-8.54	3.14	3.88
24	0	-206	17.0	-26.4	9.69	26.7
	10 ⁻⁴	-163	13.5	-21.1	7.76	21.3
	10 ⁻³	-17.2	1.43	-26.2	9.61	11.0
	10 ⁻²	-6.28	0.521	-3.07	1.13	1.65

Table 4: Copper mass loss calculated from the EQCM and coulometric measurements at 1 and 24 hours immersion at different PDTC concentrations.

t (hour)	PDTC (mol L ⁻¹)	EQCM ($\mu\text{g cm}^{-2}$)	Coulometry ($\mu\text{g cm}^{-2}$)	Δm_{Cu} ($\mu\text{g cm}^{-2}$)	$\langle j_{\text{corr}} \rangle$ ($\mu\text{A cm}^{-2}$)
1	0	-5.83	5.10	-10.9	4.81
	10^{-4}	-9.68	3.14	-12.8	5.40
	10^{-3}	14.3	1.50	12.8	-5.40
	10^{-2}	14.8	3.88	10.9	-4.60
24	0	-242	26.7	-268.7	4.73
	10^{-4}	-150	21.3	-171.3	3.01
	10^{-3}	92.6	11.0	81.6	-1.43
	10^{-2}	20.1	1.65	18.4	-0.324

Table 5: The corrosion kinetic parameters of Cu in 0.5 mol L⁻¹ NaCl in absence and in presence of PDTC at different concentrations for two different immersion times.

PDTC (mol L ⁻¹)	1 h immersion				24 h immersion			
	Blank	0.1	1	10	Blank	0.1	1	10
E_{corr} (V / SCE)	-0.271	-0.272	-0.214	-0.225	-0.226	-0.228	-0.155	-0.179
j_{corr} ($\mu\text{A cm}^{-2}$)	6.14	5.22	1.23	0.0274	3.47	4.61	0.755	0.00433
b_a (V ⁻¹)	31.6	30.7	20.4	15.5	32.6	20.1	17.9	16.8
b_c (V ⁻¹)	-27.7	-18.3	-14.0	-20.6	-49.0	-5.18	-30.8	-18.2
B (mV)	16.9	20.4	29.1	27.7	12.3	39.6	20.5	28.6

Table 6: Film capacitance C_f at 1 and 24 hour immersion and the estimation of the CuCl film thickness for Cu electrode immersed in 0.5 mol L⁻¹ NaCl in presence of different concentrations of PDTC.

PDTC (mol L ⁻¹)	1 h immersion			24 h immersion		
	C_f ($\mu\text{F cm}^{-2}$)	d (nm)	$d(Q_2)$ (nm)	C_f ($\mu\text{F cm}^{-2}$)	d (nm)	$d(Q_2)$ (nm)
0	8.65	0.77	30.5	0.731	9.1	65.2
10 ⁻⁴	9.05	0.73	12.4	56.4	0.12	52.2
10 ⁻³	0.324	20.5	9.35	0.085	78.3	64.7
10 ⁻²	0.159	41.7	21.1	0.060	110	7.6

Table 7: The inhibitive effect of PDTC at different concentrations determined by various techniques used in this study. For the blank test solution, the corrosion current density estimated by each method is shown. $d(Q_2)$ is the thickness of CuCl film calculated from coulometric results.

ImmersionTime	PDTC (mol L ⁻¹)	EQCM	EQCM+Q*	Voltammetry	EIS
1 hour	Blank (μA cm⁻²)	4.15	4.81	6.14	3.43
	10 ⁻⁴ (%)	3.13	-12.3	15.0	-9.33
	10 ⁻³ (%)	-143	212	80.0	61.7
	10 ⁻² (%)	88	196	99.6	96.0
24 hours	Blank (μA cm⁻²)	6.08	4.73	3.47	2.98
	10 ⁻⁴ (%)	75.2	36.4	-32.9	23.5
	10 ⁻³ (%)	94.3	130	78.2	96.8
	10 ⁻² (%)	99.0	107	99.9	99.7

* j_{corr} calculated by coupling EQCM and Coulometric methods